Review of Scientific Instruments

RESEARCH ARTICLE | JULY 07 2020

Frequency instability of a miniature optically pumped cesium-beam atomic frequency standard

Weibin Xie ; Qing Wang ; Xuan He; Nan Chen; Zezheng Xiong; Shengwei Fang; Xianghui Qi; Xuzong Chen

Rev. Sci. Instrum. 91, 074705 (2020)
https://doi.org/10.1063/5.0001749

Review of Scientific Instruments ARTICLE scitation.org/journal/rsi

Frequency instability of a miniature optically pumped cesium-beam atomic frequency standard

Cite as: Rev. Sci. Instrum. 91, 074705 (2020); doi: 10.1063/5.0001749
Submitted: 20 January 2020 • Accepted: 19 June 2020 •
Published Online: 7 July 2020

Weibin Xie,[1,a)] Qing Wang,[2] Xuan He,[1] Nan Chen,[1] Zezheng Xiong,[1] Shengwei Fang,[1] Xianghui Qi,[1] and Xuzong Chen[1]

AFFILIATIONS

[1]Institute of Quantum Electronics, School of Electronics Engineering and Computer Science, Peking University, Beijing 100871, China
[2]Institute of Fundamental Experiment Education, School of Electronics Engineering and Computer Science, Peking University, Beijing 100871, China

[a)]**Author to whom correspondence should be addressed:** weibinxie@pku.edu.cn

ABSTRACT

This paper proposes a miniature optically pumped cesium-beam atomic frequency standard with a volume of 38.4 l and a weight of 28 kg and examines the main factors that affect its signal-to-noise ratio (SNR). Methods to improve the SNR are proposed, which improve the short-term frequency instability: installing a collimator at the exit of the cesium oven, using the beam fluorescence spectrum with the fiber-coupled output to stabilize the laser frequency, and using the 4–5 cycling transition of the cesium D_2 line for the atomic detection. We also examine several frequency shifts that affect the long-term frequency instability and detail methods to reduce these shifts. At present, the frequency instability achieved by the Peking University miniature optically pumped cesium-beam frequency standard has reached $3.12 \times 10^{-12}/\sqrt{\tau}$.

I. INTRODUCTION

At present, the main commercial atomic frequency standards are microwave clocks, including hydrogen masers, cesium clocks, and rubidium clocks. Hydrogen masers and rubidium clocks are based on the same concept, an atomic vapor cell, which is particularly sensitive to the environment, and this limits the mid- and long-term frequency instability. In the case of a cesium-beam clock, the principle is different: the atoms are used in an atomic beam. This reduces the influence of the environment and enables better mid- and long-term frequency instability. Due to their excellent stability and other properties, the use of cesium-beam atomic clocks has become common.[1] They have been widely applied in many fields such as precision measurement, positioning and navigation, and high-speed communication.[2] The most important parameters of an atomic frequency standard are its frequency accuracy and frequency instability. As secondary frequency standards, miniature cesium-beam atomic clocks focus on frequency instability, and the main factor affecting their short-term frequency instability is the signal-to-noise ratio (SNR) of the Ramsey fringe. The various frequency shifts of an atomic clock will determine its frequency accuracy. However, the fluctuations of the frequency shifts also have a great influence on the long-term frequency instability. Therefore, a systematic study of these frequency shifts is key to improving the long-term frequency instability of atomic frequency standards.

This paper proposes a miniature optically pumped cesium-beam atomic frequency standard with a volume of 38.4 l and a weight of 28 kg and examines the main factors that affect its SNR. A method to improve the SNR of the frequency standard that enhances its short-term frequency instability is also proposed. We study the second-order Zeeman effect, which causes the largest frequency shift in an optically pumped cesium-beam atomic clock, the easily overlooked cavity-pulling and Rabi-pulling effects, and the light shift that is unique to these instruments. We detail a method to reduce the frequency shifts and describe ways to improve the long-term frequency instability.

II. EXPERIMENTAL SETUP

Figure 1 shows a schematic of the miniature optically pumped cesium-beam atomic frequency standard that is the subject of this study, including the Cesium oven, the optical pumping and detection regions, the microwave excitation regions, and the electronic system. Apart from the electronic system, all components are sealed in a vacuum tube covered by three layers of the magnetic shielding material. This is often called a cesium-beam tube. All the gaskets are made of copper, with the exception of indium seals for the windows. The tube is continuously pumped by using a titanium sublimation pump (0.3 l/s), and the operating pressure is of the order of 10^{-7} Pa.

The $F = 4 \rightarrow F' = 4$ transition of the Cs D_2 line is used for optical pumping, and the $F = 4 \rightarrow F' = 5$ transition is used for detection (Fig. 2). The radio-frequency interrogation is classically performed in a Ramsey microwave cavity, but first, the atoms have to be prepared in a single hyperfine atomic state F = 3. This preparation is performed by optical pumping instead of magnetic state selection. In this case, there is no spatial separation and all the atoms pass through the laser toward the microwave cavity. This results in a higher number of useful atoms and consequently a higher SNR than with magnetic state selection at the same oven temperature. Finally, detection of the cesium atoms is performed using the standard optical technique in the detection region. The fluorescence photons of these atoms are detected by using a photodiode.

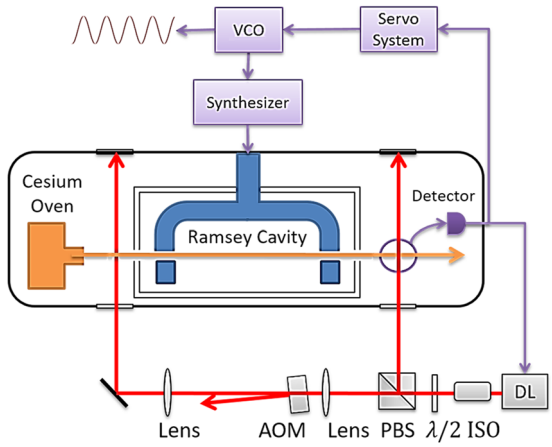

FIG. 1. Schematic of the miniature optically pumped cesium-beam atomic frequency standard.

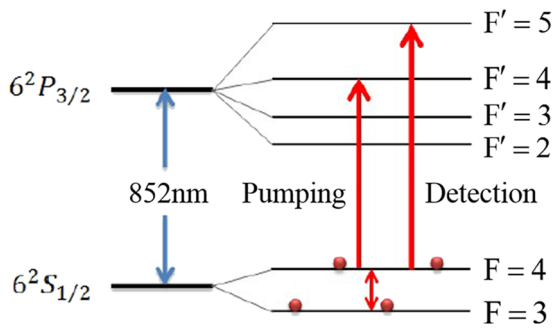

FIG. 2. Energy levels of the Cs D_2 line.

III. FACTORS AFFECTING THE SHORT-TERM FREQUENCY INSTABILITY

First, we introduce our analysis and the scheme for the control of the short-term frequency instability. The short-term frequency instability of the miniature optically pumped cesium-beam frequency standard is expressed by the Allan deviation,[3]

$$\sigma_y(\tau) = \frac{1}{\pi}\frac{\Delta\nu}{\nu_{\mathrm{hfs}}}\frac{1}{SNR}\frac{1}{\sqrt{\tau/\mathrm{s}}}. \quad (1)$$

It can be found that when the reference frequency of an atomic transition ν_{hfs} is constant, the main factors affecting the short-term frequency instability are the linewidth of the Ramsey fringe $\Delta\nu$ and the SNR. Figure 3 shows a Ramsey fringe from the instrument with a linewidth of 575 Hz and a SNR of 30 000. For a miniature cesium-beam atomic clock, it is difficult to narrow the linewidth when the volume is limited. Therefore, the Allan deviation can only be reduced by increasing the SNR. As the signals come from fluorescence resulting from the interaction between the atoms and the probe laser, we believe that there are three main parameters affecting the SNR: atomic beam intensity, laser frequency stabilization, and detection efficiency.

A. Atomic beam intensity

The most important parameter affecting the SNR is the atomic beam intensity. The number of atoms per unit length is not constant, but fluctuates. The change in the fluorescence signal caused by these fluctuations will affect the SNR.

First, we ignore the distribution of the velocities of the atoms. In the following discussion, the atomic beam intensity is I_a, the diameter of the probe laser beam is L, which will later be referred to as the "sampling length," and the time taken for the atoms to pass through the detection region (T) is called the sampling time. If the average

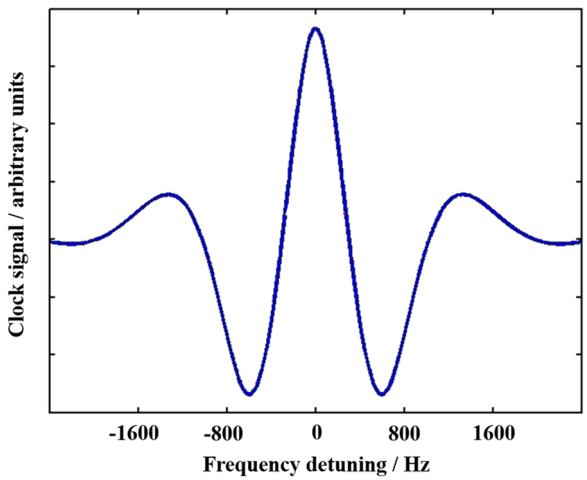

FIG. 3. Ramsey fringe from the miniature optically pumped cesium-beam atomic frequency standard.

number of fluorescent photons emitted per atom per unit time is n, then, in a region with sampling length L at any time t, the number of fluorescence photons emitted is

$$S(L,t) = n \times N(L,t), \tag{2}$$

where $N(L,t)$ is the number of atoms in the detection region at time t. If the pumping area can completely pump all atoms and all the atoms to be detected in the detection area have interacted with the microwaves, then, $N(L,t)$ can be approximated as a Poisson distribution,

$$P = [N(L,t) = \mathrm{k}] = e^{-\lambda}\frac{\lambda^{\mathrm{k}}}{\mathrm{k}!}, \quad \lambda = I_a T, \quad \mathrm{k} = 0, 1, 2, 3 \ldots. \tag{3}$$

According to the properties of the Poisson distribution, the variance and average value of $N(L,t)$ are λ. Therefore, the average value of the fluorescence signal is

$$\langle S(L,t)\rangle = \langle n \cdot N(L,t)\rangle = nI_a T. \tag{4}$$

Atomic scattershot noise is defined as the square root of the noise power spectral density of the fluorescence signal at unit Hz, and the Fourier transform of the autocorrelation function of the fluorescence noise signal is used to calculate this.

The autocorrelation function of the fluorescence noise signal is

$$\begin{aligned} R(\tau) &= n^2 I_a (T - |\tau|), \quad |\tau| \le T, \\ R(\tau) &= 0, \quad |\tau| > T. \end{aligned} \tag{5}$$

Because the actual frequency is positive, the noise power spectral density is

$$F(\omega) = 4\int_0^\infty R(\tau)\cos\omega\tau \mathrm{d}\tau = 2n^2 I_a T^2 \left(\mathrm{sinc}\left(\frac{1}{2}\omega T\right)\right)^2. \tag{6}$$

In a real circuit, the signal passes through a low-pass filter. Assuming that $\omega = 2\pi f \to 0$, then,

$$\lim_{\omega\to 0} F(\omega) = 2n^2 I_a T^2 = 2n^2 \lambda T. \tag{7}$$

Thus, the SNR (1 Hz bandwidth) can be expressed as

$$\left(\frac{S}{N}\right)_{\sqrt{\mathrm{Hz}}} = \langle S(L,t)\rangle / \sqrt{2n^2\lambda T} = n\lambda / \sqrt{2n^2\lambda T} = \sqrt{I_a/2}. \tag{8}$$

If we consider the velocity distribution of the atoms, then, $T = L\int_0^\infty \frac{f(v)}{v}\mathrm{d}v$, while[4]

$$f(v) = \frac{2v^3}{\alpha^4}\exp\left(-\frac{v^2}{\alpha^2}\right), \quad \alpha = \sqrt{2kT/m}, \tag{9}$$

where k is the Boltzmann constant, T is the oven temperature, m is the atomic mass, and v is the atomic velocity. The SNR can then be written as

$$\left(\frac{S}{N}\right)_{\sqrt{\mathrm{Hz}}} = \frac{1}{2}\sqrt{\frac{\pi}{2}I_a}. \tag{10}$$

Therefore, to improve the SNR, it is necessary to increase the number of available atoms and reduce the fluctuations in the number of atoms. There are two ways to increase the number of available atoms: one is to raise the temperature of the cesium oven and the other is to improve atomic utilization. Under the same conditions, the higher the temperature of the cesium oven, the higher the SNR. However, because the cesium atoms will be consumed more quickly at a higher temperature, this will shorten the service life of the atomic clock.

Figure 4 shows the relationship between the oven temperature and the service life of the atomic clock under the condition that the cesium content in the cesium oven is 5 g. This reveals that when the temperature of the cesium oven is 120 °C, the lifetime of the atomic clock will be only five years.

Since cesium atomic clocks are usually used for long-term accurate time measurements, their service life is very important. As such, the SNR should be improved by increasing the atomic utilization rather than raising the temperature. To achieve this, we installed a multi-channel collimator at the exit of the cesium oven. This collimator reduces the off-axis beam intensity and improves the utilization of the atomic beam. The collimator comprises a stack of crinkled foils (foil thickness 0.02 mm, channel length 4 mm, and corrugations 0.09 mm high and 0.18 mm wide), which is equivalent to a series of densely packed slender round channels, so atoms that reach the exit at a large angle will hit the walls of the channel. The atomic beam divergence is 40 mrad. According to the results of a previous study,[5] the atomic collisions in the channels are negligible for usual temperatures and the on-axis velocity distribution is not modified by the channels. The cross-sectional dimension of the collimator is $6 \times 0.5\ \mathrm{mm}^2$, it is calculated that when the oven temperature is 100 °C, and 4.13×10^{13} cesium atoms are ejected every second from the cesium oven,[6] which is more than that (3.46×10^{13} atoms/s) obtained by other researchers at a higher oven temperature.[7]

In addition to the use of a collimator, a stable cesium atom beam should be realized to reduce fluctuations in the number of atoms and improve the frequency instability of the clock. Figure 5 shows changes in the oven temperature over time in our cesium clock. It can be seen that the temperature only varies within 1 mK, indicating a very stable control over the oven temperature.

B. Laser frequency stabilization

The lasers used for optical pumping and detection in the cesium atomic clock need to be stabilized to atomic transition lines for several years or even longer without losing the lock. In addition, the

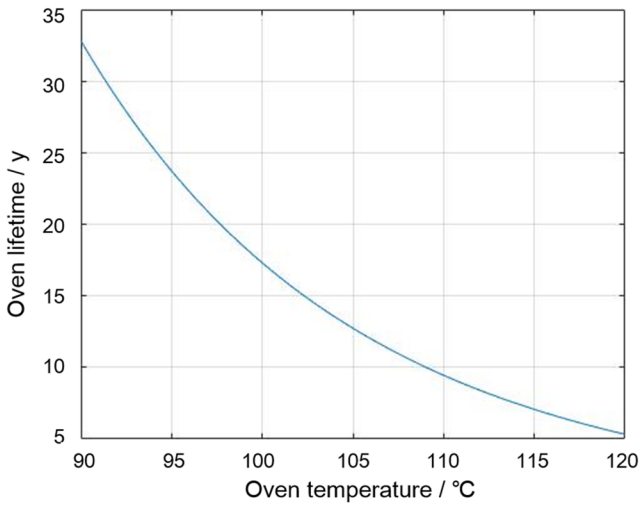

FIG. 4. The relationship between oven temperature and cesium oven life when the cesium content is 5 g.

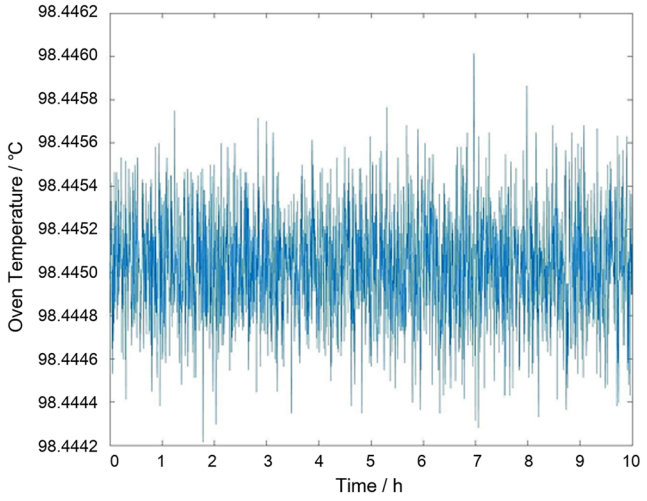

FIG. 5. Changes in the oven temperature over time.

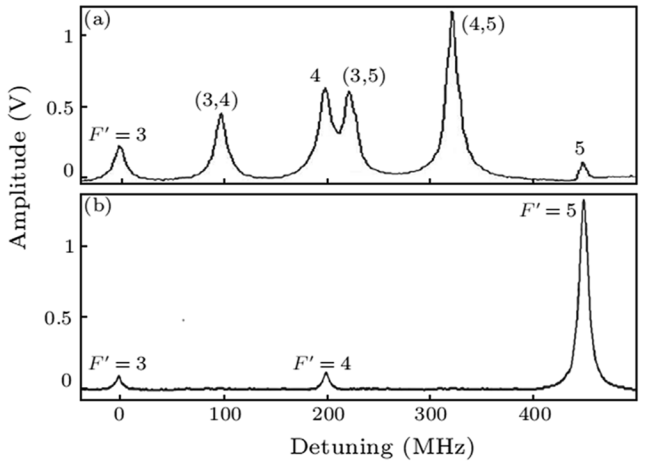

FIG. 6. The contrast between (a) saturated absorption spectroscopy and (b) beam fluorescence spectroscopy.

frequency stabilization system should not be complicated. To meet these requirements, saturated absorption spectroscopy (SAS) with the modulation of light is a common choice.[8] To improve the frequency instability, the cell temperature needs to be stabilized. Other sources of limitations such as the light density, the magnetic field, and the background gas contamination in the cell should also be taken into consideration.[9,10] However, it is difficult and complicated to control all these factors when using the SAS scheme.

Another, more stable and robust, atomic transition spectrum can be conveniently used to stabilize the laser frequency in an optically pumped cesium-beam standard. In the detection area, before interacting with the laser, the atomic beam will have passed through the pumping and microwave areas, which is equivalent to the additional collimation of the atomic beam. Thus, the divergence of the atomic beam is calculated to be less than 1°, which is small enough to be ignored. As described above, all the physical components are enclosed in the cesium-beam tube, which is covered by three layers of the magnetic shielding material, and the oven temperature is well controlled. In addition, unlike the atoms in the cell, the atomic beam is always fresh and free from background gas contamination.

Therefore, compared with the SAS method, almost all the sources of limitations to the frequency instability are eliminated. When resonances occur, the fluorescence light is collected by using a ball-shaped collector (see Fig. 1) and directed to a photodiode. Figure 6 shows fluorescence spectra from (a) SAS and (b) our system. In our system, there are three spectral lines, which correspond to the $F = 4 \rightarrow F' = 3$, 4, and 5 transitions of the Cs D_2 line. Furthermore, the spectrum is Doppler-free and without additional crossing peaks as in SAS, which is desirable to avoid detrimental cross-influences. These are, therefore, better reference lines for locking the laser frequency in our atomic clock. Due to the fact that the $F = 4 \rightarrow F' = 5$ line is a cycling transition and its strength factor is larger than those of the other two transitions, the signal of the $F = 4 \rightarrow F' = 5$ transition line is the largest.

The laser frequency is modulated by its injection current at 10 kHz and locked on the pumping transition lines $F = 4 \rightarrow F' = 5$. The modulation depth is 1 MHz. Because the SNR of the beam fluorescence spectroscopy is high, the modulation depth can be set lower, thereby reducing the effect of modulation broadening. The primary differential signal of the beam spectrum is obtained using a custom-made phase detector circuit, and frequency stabilization of the laser is performed with this signal.

In addition, we minimize the drift of the light angle by using a fiber-coupled output.[11] By locking the laser frequency to the fluorescence spectrum of the atomic beam with the fiber-coupled output, we can improve the stability of the laser frequency greatly (see Fig. 7). The stability is about 3.5×10^{-11} at 1 s, and the Allan deviation keeps decreasing with a $\sqrt{\tau}$ slope for integration times even up to

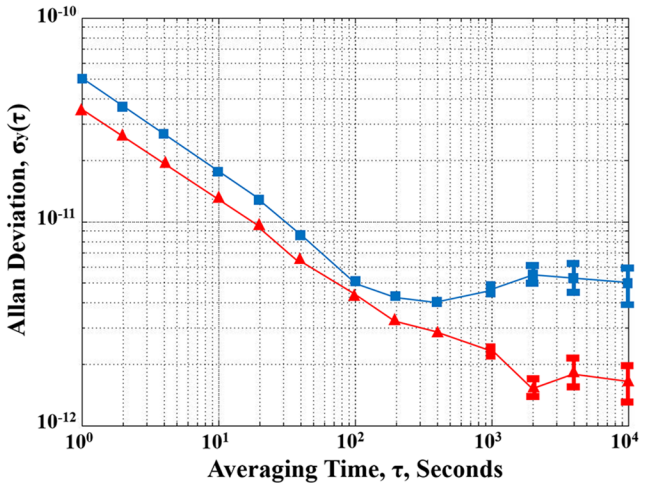

FIG. 7. Relative laser frequency stability in terms of the Allan deviation. Here, squares with the blue line represent the stability by using SAS after taking control of the cell temperature and triangles with the red line represent the stability by using the fluorescence spectrum of the atomic beam with the fiber-coupled output.

2000 s, with a flicker floor at the level of about 1.6×10^{-12}, which perfectly meets the requirement for the optically pumped cesium-beam standard.[11]

C. Detection efficiency

Detection efficiency refers to the probability that an atom in the detection area can be detected. Our system uses the light-detection method with a detection laser diameter of 6 mm and a power of 1 mW. Therefore, each atom is able to interact with the detection laser, and the detection efficiency can be expressed as the mean number of fluorescence photons emitted per atom (β) in the detection area multiplied by the fluorescence collection efficiency (η). β is generally given by[12]

$$\beta = \Gamma T_{\mathrm{m}} \langle \Pi_e \rangle, \tag{11}$$

where Γ is the rate of the radiative deexcitation, T_{m} is the mean interaction time, and Π_e is the stationary population of the excited state e. Equation (11) is valid if we assume that the duration of the transient evolution of the atomic state (a few Γ^{-1}) is negligible compared to T_{m}. This is generally true for conventional interactions of laser with thermal atomic beam.[13] In our case, because the F = 4 → F′ = 5 line is a cycling transition, $\beta = 240$ and $\eta = 32\%$,[2] so $\beta\eta \gg 1$. In other words, the detection efficiency is 100%.

IV. FACTORS AFFECTING THE LONG-TERM FREQUENCY INSTABILITY

Several reports indicate that the long-term frequency instability of a conventional magnetic-state-selection cesium clock is mainly determined by the microwave power drift.[14–17] However, in optically pumped cesium-beam frequency standards, the long-term frequency instability is affected not only by the microwave power drift but also by the light shift.[18] In addition, there is a frequency shift caused by the second-order Zeeman effect, and this is the largest frequency shift in an optically pumped cesium-beam atomic clock.

A. Second-order Zeeman effect

To generate the cesium atom's $|F = 3, m_F = 0\rangle \rightarrow |F = 4, m_F = 0\rangle$ transition line, where F indicates the ground-state hyperfine levels and m_F is the magnetic quantum number of the initial and final states, a weak and static magnetic field called a C field is used to generate the Zeeman split (Fig. 8). If the intensity of the C field is

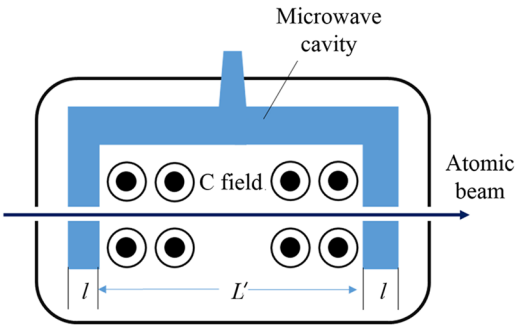

FIG. 8. The microwave cavity of the cesium-beam frequency standard.

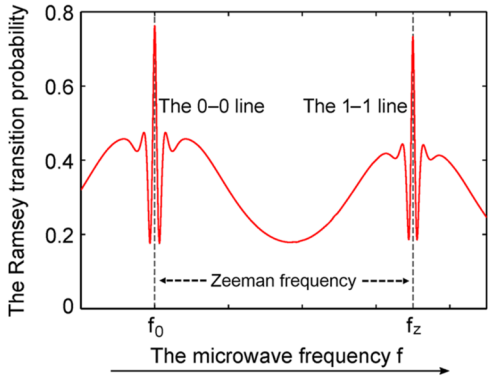

FIG. 9. The 0–0 transition line and the 1–1 transition line of the Ramsey fringe.

B_0, according to the Breit–Rabi formula,[19] the frequency shift of the $|F = 3, m_F = 0\rangle \rightarrow |F = 4, m_F = 0\rangle$ transition line caused by the C field is

$$\Delta\nu_z = \frac{1}{2\nu_{\mathrm{hfs}}} \frac{(g_J + g_I)\mu_{\mathrm{B}}^2}{h^2} B_0^2 \approx 427.45 \times 10^8 B_0^2, \tag{12}$$

where g_J and g_I are the g factors for the atom and the nucleus, respectively, μ_{B} is the Bohr magneton, $x = (g_J + g_I)\mu_{\mathrm{B}} B_0 / E_{\mathrm{hfs}}$, and E_{hfs} is the unperturbed cesium hyperfine separation. According to Eq. (12), the shift is only related to the square of the intensity of the C field, so the shift is called a second-order Zeeman effect. When the C field is 60 mGs, the relative shift is 1.674×10^{-10}, which, as noted, is the largest shift in an optically pumped cesium atomic clock.

The intensity of the C field is generally controlled by locking the Zeeman frequency. Scanning the microwave frequency can obtain the 1–1 transition line adjacent to the 0–0 transition line (Fig. 9). The frequency difference Δf between the 1–1 line and the 0–0 line is the Zeeman frequency. Since the C field is generated by passing current through a coil, the C-field current is proportional to the C-field strength and the Zeeman frequency is linearly related to the C-field strength. Therefore, we adjusted the microwave frequency to $f_0 + \Delta f \pm f_{\mathrm{m}}$, where f_{m} is the modulation depth. In the same way as the microwave frequency servo-control principle, the error signal is fed back to the C-field current to achieve stable control. The locking accuracy of the C-field intensity can reach 1.6×10^{-5}, as shown in Fig. 10, meaning that the second-order Zeeman frequency shift has only a small impact on the long-term frequency instability of the order of 10^{-15}. We assign an instability budget of $2.7 \times 10^{-15} \nu_{\mathrm{hfs}}$ to this effect.

B. Microwave power drift

A cesium-beam atomic clock uses a special microwave cavity to obtain the Ramsey fringe, and the Ramsey fringe can be used to lock the frequency of the crystal oscillator. In the microwave region, the cesium atoms pass through the first interaction zone with length l, the free-evolution zone with length L', and the second interaction zone. For an atom of speed v, the time taken to travel through the interaction zone is $\tau = l/v$ and the time taken to travel through the free-evolution zone is $T = L'/v$.

In the process of calculating the Ramsey transition probability using the Schrödinger equation, the microwave field is assumed to

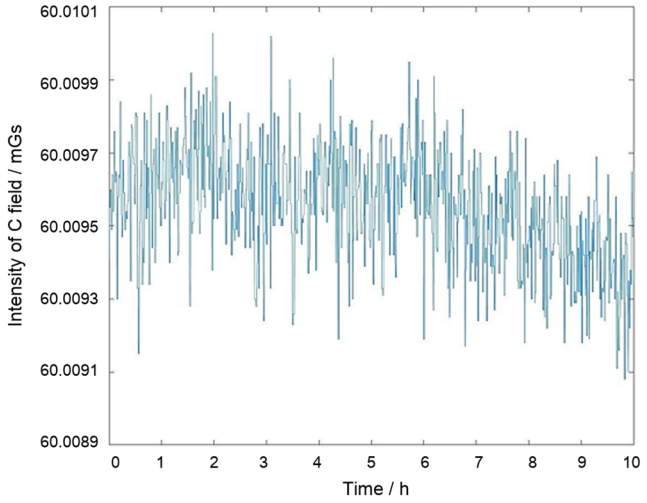

FIG. 10. Changes in the intensity of the C field with time.

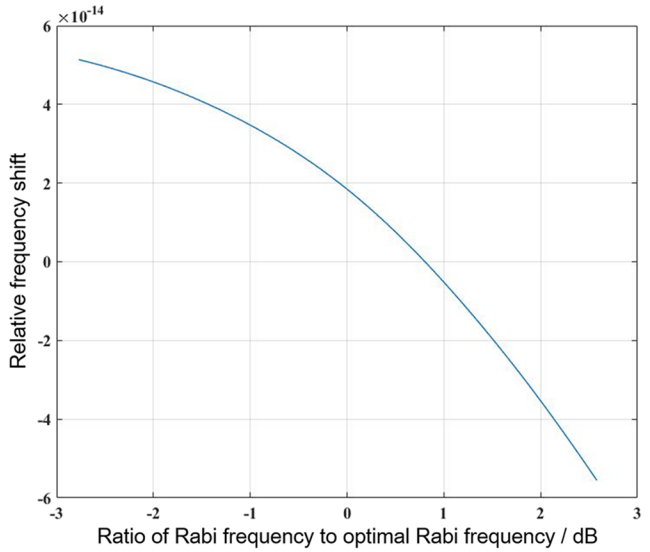

FIG. 11. Relationship between the microwave power and the relative frequency shift caused by the cavity-pulling effect.

be

$$B(t) = B\cos(\omega t + \phi). \tag{13}$$

The perturbation introduced by the microwave field is then

$$V_{|4,0\rangle-|3,0\rangle} = b\cos(\omega t + \phi), \tag{14}$$

where $b = \mu_B B/\hbar$ is the Rabi frequency.

1. Cavity-pulling effect

In the actual microwave cavity, the amplitude of the microwave field is modified due to the different responses of the cavity to different microwave frequencies, so b also becomes a function of the amount of detuning Δ. If the cavity resonance frequency is not exactly tuned to the atomic transition frequency, b varies asymmetrically with Δ. Therefore, this amplitude contains components that produce a frequency shift in the measured transition frequency. This is known as cavity pulling.

In a cesium-beam atomic clock with slow square-wave modulation, the servo system will separately acquire the Ramsey signal at $\omega = \omega_c - \omega_m$ and $\omega = \omega_c + \omega_m$, where ω_c is the center angular frequency of the cavity and ω_m is the modulation depth, and use the difference between the two signals as the error signal to adjust ω. When the error signal is zero, $\omega = \omega_c$. For small cavity mistuning, the relative frequency shift caused by cavity pulling is[20]

$$\frac{\omega_{CP} - \omega_0}{\omega_0} = 2bT_c^2\omega_m \times \frac{\omega_c - \omega_0}{\omega_0}\frac{\int_0^\infty \tau \sin b\tau \cos b\tau (1 + \cos\omega_m T) f(\tau) d\tau}{\int_0^\infty f(\tau) T \sin^2 b\tau \sin\omega_m T d\tau}, \tag{15}$$

where T_c is the time constant of the microwave cavity, ω is the angular frequency of the microwaves, and $f(\tau)$ is the speed distribution of the cesium atoms. For our optically pumped cesium atomic clock,

$$f(\tau) = \frac{4}{\sqrt{\pi}}\frac{\tau_0^3}{\tau^4}\exp(-\tau_0^2/\tau^2), \tag{16}$$

where $\tau_0 = l/\alpha$ in which $\alpha = \sqrt{2kT/M}$ is the most probable speed, k is the Boltzmann constant, T is the oven temperature, and M is the mass of a cesium atom.

We use Eq. (15) to study the properties of cavity pulling. In our optically pumped atomic clock, the quality factor of the microwave cavity is $Q_c = 500$, the cavity mistuning is $\omega_c - \omega_0 = 2\pi \times 500$ krad/s, the oven temperature is 100 °C, the length of the free-evolution zone is $L' = 177$ mm, and the length of the interaction zone is $l = 10$ mm. There is a particular microwave power at which the amplitude of the Ramsey fringe is the largest, and this value is called the optimal microwave power. The Rabi frequency corresponding to this power is $b_{opt} \approx 37\,100$ rad/s.

The influence of the microwave power on cavity pulling can be studied by controlling other conditions and changing the value of the Rabi frequency b. The results of these calculations are shown in Fig. 11.

It can be seen from Fig. 11 that at the optimal microwave power, the relative frequency shift caused by cavity pulling is 1.81×10^{-14} and the slope around the optimal microwave power is -2×10^{-14} dB^{-1}. As the microwave power increases, the relative frequency shift will pass through the zero point. Therefore, in actual operation, appropriately increasing the microwave intensity can eliminate the influence of cavity pulling without significantly reducing the Ramsey signal amplitude.

2. Rabi-pulling effect

When the cesium atoms pass through the microwave field, in addition to the clock transition $|F = 3, m_F = 0\rangle \rightarrow |F = 4, m_F = 0\rangle$, the adjacent two π transitions, $|F = 3, m_F = -1\rangle \rightarrow |F = 4, m_F = -1\rangle$ and $|F = 3, m_F = 1\rangle \rightarrow |F = 4, m_F = 1\rangle$, will also occur and there will be two Rabi pedestals. If the strength of the C field is insufficient, resulting in insufficient Zeeman splitting, then, the tails of the Rabi pedestals will extend to the position of the clock transition and be

superimposed with the clock transition's Ramsey signal, which will become the actual Ramsey transition probability. If the strengths of two adjacent transition lines are not equal because of the beam optics or other factors, the center frequency of the $|F = 3, m_F = 0\rangle \rightarrow |F = 4, m_F = 0\rangle$ transition line will move.

The relative frequency offset caused by Rabi pulling is[21]

$$\frac{\Omega_{Rabi}}{\omega_0} = \frac{15}{8\sin^2 b\tau} \frac{\varepsilon b^2 (2\varepsilon^2 - (15/16)b^2)}{\omega_0 T^2 (\varepsilon^2 + (15/16)b^2)^3} \frac{n_1 - n_{-1}}{n_0}, \quad (17)$$

where n_1 and n_{-1} are the strengths of the $|F = 3, m_F = -1\rangle \rightarrow |F = 4, m_F = -1\rangle$ and $|F = 3, m_F = 1\rangle \rightarrow |F = 4, m_F = 1\rangle$ transition lines, respectively, and n_0 is the strength of $|F = 3, m_F = 0\rangle \rightarrow |F = 4, m_F = 0\rangle$. In our optically pumped cesium atomic clock, $\frac{n_1 - n_{-1}}{n_0} = 0.0075$ and the Zeeman frequency is $\varepsilon = 2\pi \times 45$ krad/s.

We use Eq. (17) to study the properties of the Rabi-pulling effect. The influence of the microwave power on the Rabi pulling can be studied by controlling other conditions and changing the value of the Rabi frequency b. The results of these calculations are shown in Fig. 12.

It can be seen from Fig. 12 that the relative frequency offset caused by the Rabi-pulling effect increases with the microwave power. At the optimum microwave power, the relative frequency shift caused by Rabi pulling is 4.52×10^{-14} and the slope around the optimal microwave power is -1.31×10^{-14} dB^{-1}.

Therefore, stable microwave power is very important. However, changes in the external environment will affect the microwave power and fluctuations in the microwave power will lead to the deformation of the Ramsey fringe. The frequency shifts caused by cavity pulling and Rabi pulling will also then change, thus worsening the frequency instability. Therefore, we apply active servo control to the microwave power to maintain it at a stable value. The microwave power fractional fluctuations do not exceed 4×10^{-3}, so we assign an instability budget of $7 \times 10^{-17} \nu_{hfs}$ to cavity pulling and $1.8 \times 10^{-16} \nu_{hfs}$ to Rabi pulling.

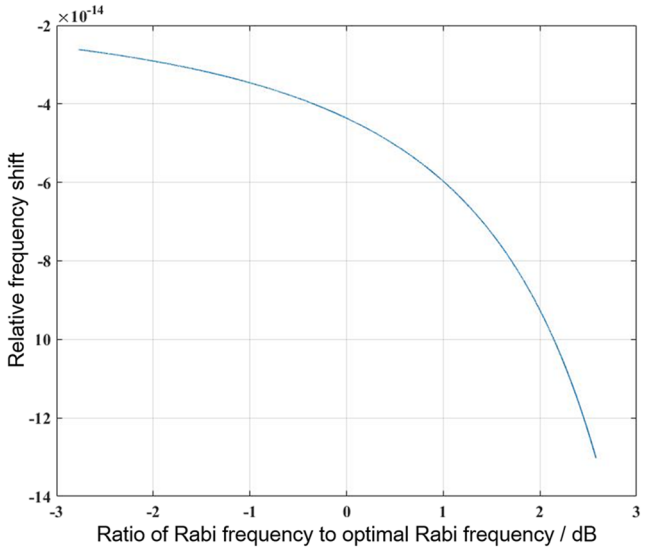

FIG. 12. Relationship between the microwave power and the relative frequency shift caused by the Rabi-pulling effect.

C. Light shift

In an optically pumped cesium-beam atomic clock, the influence of light shift cannot be ignored. This is because the state preparation and the detection of cesium atoms are realized by the interaction with the laser and the fluorescence generated in these two processes may leak into the microwave cavity and produce a second-order Stark shift in the cesium atoms that will cause the frequency of the atomic clock to shift. The influence of the light power on the light shift is measured by manually changing the incident light power and then testing the output frequency of the frequency standard.

As can be seen from Fig. 13, when the laser power is weak, the frequency shift linearly increases with the laser power. However, when the laser power reaches a certain value, the upward slope of the light shift increases sharply. This can be explained by the fact that increasing the laser power increases the beam diameter, resulting in the nonlinear enhancement of the scattered light.

Through linear fitting of the sampled data, the relative frequency shift caused by the detection light was found to be 4.351×10^{-13} mW^{-1}. By the same method, the relative frequency shift caused by the pumping light was established as -2.176×10^{-13} mW^{-1}. The power of the pumping light and the detection light is 2 mW, so the total light shift is 4.351×10^{-13}. Therefore, it is very important to achieve stable control of the laser power.

In the miniature optically pumped cesium-beam atomic frequency standard, a combination of a single laser and an acousto-optic modulator (AOM) is used to realize optical pumping and detection (see Fig. 1). In this way, the laser frequency can be locked using the working current and its power can be controlled by using the AOM and feedback circuit. At present, the laser power fractional fluctuations can be controlled below a factor of 10^{-3}, so we assign an instability budget of $4 \times 10^{-16} \nu_{hfs}$ to this effect.

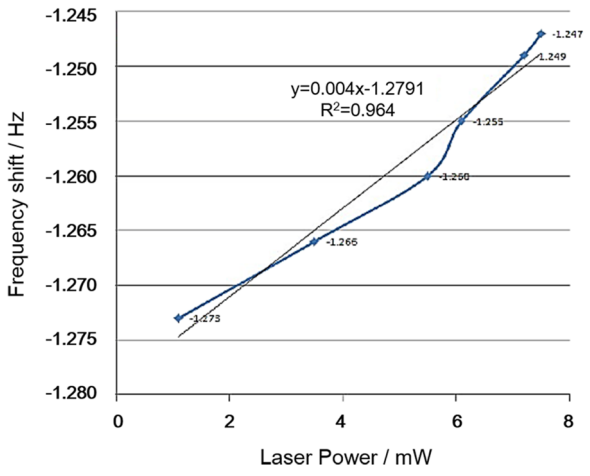

FIG. 13. Relationship between frequency shift and detection light power.

D. Other frequency shifts

We also examined several other frequency shifts, which have been studied in more detail in previous research studies,[22–24] so we will only give a brief summary of these here.

1. Second-order Doppler frequency shift

In an optically pumped cesium-beam atomic clock, the first-order Doppler shift is negligible because the direction of the cesium atoms is perpendicular to the direction of the microwave field. However, due to the time-expansion effect of the theory of relativity, a second-order Doppler shift is generated. Under our experimental conditions, the second-order Doppler shift is about -3.771×10^{-13} and the rate of change at the optimal microwave power is -3.91×10^{-14} dB^{-1}, which is basically proportional to the oven temperature. The slope is -1.06×10^{-15}/°C. Since the fluctuations in the temperature of our oven can be controlled within ±0.1 °C, this frequency shift has a little effect on the long-term frequency instability. We assign an instability budget of $1 \times 10^{-16} \nu_{\mathrm{hfs}}$ to this effect.

2. Black-body shift

When a cesium atom travels through a microwave cavity, it is affected by the black-body radiation generated by the surrounding environment and the radiation field causes the atomic energy levels to move. At our working temperature $T = 308$ K, the black-body shift is -1.91×10^{-14} and the rate of change with ambient temperature is -2.50×10^{-16} K^{-1}. As the atomic clock is placed in a room whose temperature does not change by more than 1 K, this kind of frequency shift has less effect on the long-term frequency instability. We assign an instability budget of $2.5 \times 10^{-16} \nu_{\mathrm{hfs}}$ to this effect.

V. DISCUSSION AND CONCLUSIONS

This paper examined the main factors that affect the SNR of a miniature optically pumped cesium-beam atomic frequency standard, and the following three methods for improving the SNR are proposed:

(1) Installing a collimator at the exit of the cesium oven.
(2) Using the beam fluorescence spectrum instead of saturated absorption spectroscopy to stabilize the laser frequency.
(3) Using the $F = 4 \rightarrow F' = 5$ cycling transition line for detection to achieve 100% detection efficiency.

We also studied the second-order Zeeman effect, which causes the largest frequency shift in the optically pumped cesium-beam atomic clock, the easily overlooked cavity-pulling and Rabi-pulling effects, and the characteristic light shift. Based on the study of these frequency shifts, we believe that the following ways are beneficial for improving the long-term frequency instability:

(1) To reduce the instability budget caused by the second-order Zeeman effect, we stabilized the intensity of the C field by locking the Zeeman frequency, in the same way as the microwave frequency servo-control principle.
(2) To reduce the instability budget caused by the cavity-pulling effect and Rabi-pulling effect, we controlled the microwave power by applying active servo control to the microwave power.

TABLE I. Relative frequency shifts and their instability budgets.

Effect	Relative shifts in parts in 10^{16}	Instability budgets in parts in 10^{16}
Second-order Zeeman	167 400	27
Cavity pulling	181	0.7
Rabi pulling	−452	1.8
Light shift	4 351	4
Second-order Doppler	−3771	1
Black-body radiation	−191	2.5
Total	167 518	27.5

(3) To reduce the instability budget caused by the light shift, we controlled the laser power by using the AOM and feedback circuit.

Table I summarizes all the frequency shifts that were considered and lists their corresponding instability budgets under our experimental conditions.

Figure 14 shows the Allan deviation of the Peking University optically pumped cesium-beam frequency standard measured against the reference hydrogen maser (VCH-1008, VREMYA-CH). A picosecond resolution instrument (PicoTime-1U, Orolia) was used to perform the frequency comparison. The frequency instability reached $3.12 \times 10^{-12}/\sqrt{\tau}$, exceeding the 5071 A high-performance tube (Symmetricom), and is comparable with the OSA 3300 (Oscilloquartz SA). According to Table I and the short-term frequency instability, we predict that the flicker floor will be around 3×10^{-15} under our experimental conditions. In the future, we will continue to measure the long-term frequency instability and complete the engineering of this optically pumped cesium-beam frequency standard. A miniature optically pumped cesium-beam atomic frequency standard with a volume of 38.4 l and a weight of 28 kg has now been successfully manufactured (Fig. 15).

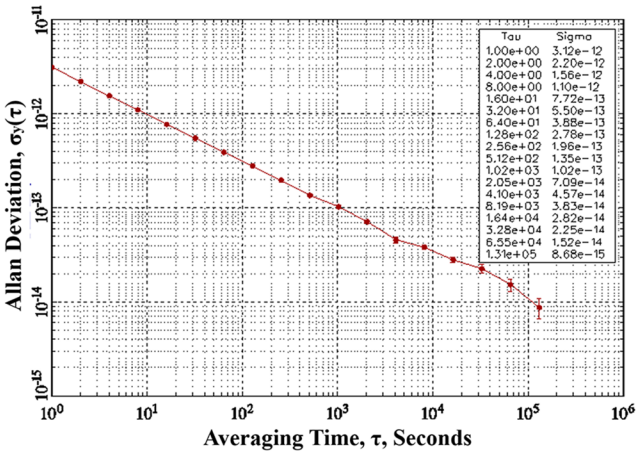

FIG. 14. The Allan deviation of the Peking University optically pumped cesium-beam frequency standard measured against the reference hydrogen maser.

FIG. 15. The Peking University optically pumped cesium-beam frequency standard.

ACKNOWLEDGMENTS

The authors would like to thank the Advanced Technology Institute of Peking University for its support of this research.

DATA AVAILABILITY

The data that support the findings of this study are available from the corresponding author upon reasonable request.

REFERENCES

[1]Y. Q. Wang, Q. J. Wang, J. S. Fu, and T. Q. Dong, *The Principle of Quantum Frequency Standards* (Science Press, Beijing, 1986).
[2]Q. Wang, "Research on miniature optically pumped cesium beam frequency standard," Ph.D. thesis, Peking University, 2014.
[3]F. Riehle, *Frequency Standards* (Wiley-VCH Verlag GmbH, Weinheim, 2004).
[4]J. Vanier and C. Audoin, *The Quantum Physics of Atomic Frequency Standards* (A. Hilger, Philadelphia, 1989).
[5]E. de Clercq, A. Clairon, B. Dahmani, A. Gérard, and P. Aynié, *Frequency Standards and Metrology* (Springer-Verlag, Berlin, 1989).
[6]W. B. Xie, Q. Wang, X. He, X. H. Qi, and X. Z. Chen, in Joint Conference of the IEEE International Frequency Control Symposium and IEEE International Symposium on Applications of Ferroelectrics, Keystone, CO, USA, 2020.
[7]H. Shi, J. Ma, X. F. Li, J. Liu, and S. G. Zhang, Appl. Opt. **57**, 6620 (2018).
[8]G. D. Rovera, G. Santarelli, and A. Clairon, Rev. Sci. Instrum. **65**, 1502 (1994).
[9]C. Affolderbach and G. Mileti, Rev. Sci. Instrum. **76**, 073108 (2005).
[10]G. P. Barwood, P. Gill, and W. R. C. Rowley, Appl. Phys. B **53**, 142 (1991).
[11]Q. Wang, J. Duan, X.-H. Qi, Y. Zhang, and X.-Z. Chen, Chin. Phys. Lett. **32**, 054206 (2015).
[12]S. Reynaud, Ann. Phys. **8**, 315 (1983).
[13]N. Dimarcq, V. Giordano, and P. Cerez, Appl. Phys. B **59**, 135 (1994).
[14]C. Audoin, F. Hamouda, L. Chassagne, and R. Barillet, IEEE Trans. Ultrason., Ferroelectr., Freq. Control **46**, 407 (1999).
[15]C. Audoin, N. Dimarcq, V. Giodano, and J. Viennet, IEEE Trans. Ultrason., Ferroelectr., Freq. Control **39**, 412 (1992).
[16]A. D. Marchi, G. D. Rovera, and A. Premoli, Metrologia **20**, 37 (1984).
[17]A. D. Marchi, IEEE Trans. Ultrason., Ferroelectr., Freq. Control **34**, 598 (1987).
[18]A. Brillet, Metrologia **17**, 147 (1981).
[19]N. F. Ramsey, *Molecular Beams* (Clarendon Press, Oxford, 1956).
[20]C. Audoin, P. Lesage, and A. G. Mungall, IEEE Trans. Ultrason., Ferroelectr., Freq. Control **23**, 501 (1974).
[21]H. S. Lee, T. Y. Kwon, H.-S. Kang, Y.-H. Park, C.-H. Oh, S. E. Park, H. Cho, and V. G. Minogin, Metrologia **40**, 224 (2003).
[22]A. Makdissi and E. D. Clercq, Metrologia **38**, 409 (2001).
[23]J. H. Shirley, W. D. Lee, and R. E. Drullinger, Metrologia **38**, 427 (2001).
[24]K. Hagimoto, S. Ohshima, Y. Nakadan, and Y. Koga, IEEE Trans. Instrum. Meas. **48**, 496 (1999).